IEEE Access
Multidisciplinary | Rapid Review | Open Access Journal

Date of publication xxxx 00, 0000, date of current version xxxx 00, 0000.

Digital Object Identifier 10.1109/ACCESS.2017.DOI

Common-Mode Voltage Mitigation of Dual Three-phase Voltage Source Inverters in a Motor Drive Application

ABRAHAM MARQUEZ ALCAIDE[1], (Member, IEEE), XUCHEN WANG[2], (Member, IEEE), HAO YAN[3], (Member, IEEE), JOSE I. LEON[1,4], (Fellow, IEEE) VITO G. MONOPOLI[5], (Member, IEEE) GIAMPAOLO BUTICCHI[2], (Member, IEEE) SERGIO VAZQUEZ[1], (Fellow, IEEE), MARCO LISERRE[6], (Fellow, IEEE), LEOPOLDO G. FRANQUELO[1,4], (Life Member, IEEE)

[1]Universidad de Sevilla, 41092, Spain (e-mail: amarquez@ieee.org)
[2]University of Nottingham - Ningbo China, Electrical and electronic Engineering, Ningbo, Zhejiang, 315100, China
[3]School of Civil Aviation, Northwestern Polytechnical University, Xi'an, China
[4]Departament of Astronautic, Harbin Institute of Technology, 15001, Harbin, China
[5]Politecnico di Bari, Departement of Electrical and Information Engineering, Bari, 70126, IT
[6]Christian-Albrechts-Universität zu Kiel, Kiel, DE

Corresponding author: Xuchen Wang (e-mail: xuchen.wang@nottingham.edu.cn).

The authors gratefully acknowledge the financial support provided by the H2020 Spartan project (ID 821381), the Spanish Science and Innovation Ministry under project TEC2016-78430-R, the Consejería de Economía, Conocimiento, Empresas y Universidad. Secretaría General de Universidades, Investigación y Tecnología under the project PY18-1340

ABSTRACT Electric variable speed drives (VSDs) based on two VSDs connected to a multiphase machine are an attractive solution to replace high-power mechanic and hydraulic systems in many sectors of industry and transportation because they present high performance with reduced cost, volume and weight. Among the causes which affect the reliability of dual VSDs, the common-mode current flowing through the machine bearing is an important issue. This paper faces the mitigation of the common-mode current by reducing the common-mode voltage (CMV) generated by the operation of a dual VSD. The CMV reduction is carried out without introducing any extra device and/or passive filtering method. This CMV reduction is performed by applying a specific phase-displacement between the modulation strategies of each single inverter drive. The proposed technique has been evaluated in a down scaled experimental setup in order to test its effectiveness.

INDEX TERMS Harmonic analysis, Pulse width modulation, Common-mode voltage.

I. INTRODUCTION

The industry is moving from mechanical and hydraulic systems to the electrical drives because they present a better performance with a cost reduction [1]. As an example, permanent magnet synchronous machines (PMSMs) are widely used in electric vehicles owing to their advantages such as high efficiency, reduced cost and high performance [2], [3]. In order to achieve these objectives, the efficient and reliable variable speed drives (VSDs) are critical components of the system. In particular, the use of VSDs in power conversion systems presents many advantages such as high efficiency and superior dynamic performance because of its better control of machine flux and currents.

In recent years, the multi-phase electric machines have attracted a lot of attention and the dual three-phase machine is the most common structure among the multi-phase machine ones [4], [5]. In a dual three-phase machine, two sets of three-phase stator windings increase the fault-tolerant ability and make the integration with conventional three-phase technology relatively simple [6]. Among the applications, it is possible to find multi three-phase systems and more particularly the dual three-phase drive in aerospace and marine applications [7].

Power converters for VSD applications have been intensively developed in the last decades [8], [9]. New multilevel power converter structures have been proposed and advanced control strategies and modulation techniques have been explored [10], [11]. However, although these converter

This article has been accepted for publication in a future issue of this journal, but has not been fully edited. Content may change prior to final publication. Citation information: DOI 10.1109/ACCESS.2021.3072967, IEEE Access

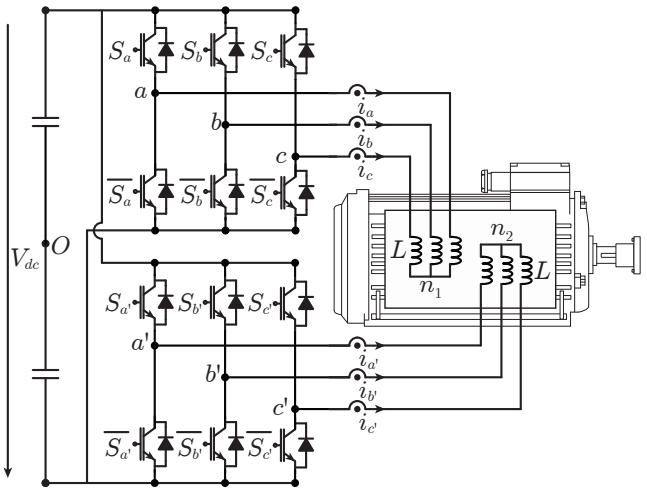

FIGURE 1: Dual-drive of a multi-phase PMSM using two three-phase two-level inverters

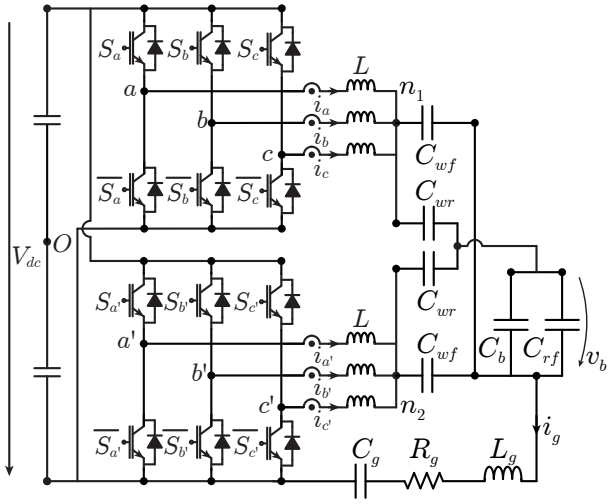

FIGURE 2: Equivalent circuit model of the motor shaft voltage

topologies are available, the penetration in the industry is still limited. The traditional three-phase two-level power converter is nowadays leading the market in most industrial solutions. As an example, in Fig. 1 a dual-drive for a multi-phase motor using two three-phase two-level inverters is shown.

In the literature, many strategies to control a VSD can be found. Among them, the direct torque control (DTC), field oriented control (FOC) or model predictive-based control are very well-known [12], [13]. In the modulation stage, the methods to operate a three-phase two-level converter can be categorized in two main groups: space vector modulations (SVM) and carrier-based pulse-width modulation (CB-PWM) techniques [10]. Most of available control platforms include a dedicate peripheral to deploy and use the PWM modulation. Therefore, CB-PWM technique is the simplest and most straight-forward way to operate the power converter.

Although the use of VSDs presents many advantages, several drawbacks directly affect to the performance, reliability and the remaining lifetime of the system [14]–[16]. As a main concern, the common-mode voltage (CMV) generated by the drive is closely related to the system reliability because of the corresponding bearings degradation. In fact, it has been demonstrated that the CMV is the cause of more than 50% of cases of motor failures [14], [15], [17]. In addition, the shaft voltage and bearing current phenomena also appear in induction machines [18], [19]. As a result of these issues, there is a trend to develop an accurate-enough mathematical approach to estimate and predict an early failure of the machine components [20]–[23].

Bearing degradation through CMV has attracted the attention of researchers in the last years. Multiple approaches have been performed, which can be categorized in two main streams: the CMV filtering via the introduction of external elements and the CMV mitigation considering a proper control strategy and/or modulation technique. Considering the introduction of external elements, passive filtering and the use of active canceler circuits can be found [24]–[27]. Despite of these methods provide good results, the introduction of extra passive filtering elements and/or active devices is undesirable because the increase in cost, volume and weight. On the other hand, if the CMV mitigation is performed by developing new modulation methods, the academia provides several options, most of them based on the proper switching pattern selection using specific SVM techniques [17], [28]–[31]. In [32], [33], the CMV mitigation for the dual drive is achieved applying a SVM method at the expense of developing complex calculations in the modulation stage.

This work studies the CMV present in the dual drive application shown in Fig. 1 and develops a simple CB-PWM method to mitigate its negative effects on the system. To perform this analysis, the CMV harmonic spectrum based on double Fourier description is carried out. From this analysis, a phase-shift between the PWM operation of both drives is proposed in order to minimize the CMV harmonic distortion. In the proposed method, the CMV mitigation is obtained without external passive filtering elements and/or active CMV canceler circuits. In addition, the proposed technique is easily implementable on the most off-the-shelf mid-range micro-controller control platforms.

The rest of the paper is organized as follows: in section II the negative effects of the CMV over the motor bearing and its degradation is presented. Section III analyzes the harmonic spectrum of the CMV as consequence of the dual drive operation. In section IV, the effect of the proposed modulation technique in the machine currents is shown. In section V, the validation of the modulation technique via experimental results is performed and section VII highlights the conclusions of the work.

This article has been accepted for publication in a future issue of this journal, but has not been fully edited. Content may change prior to final publication. Citation information: DOI 10.1109/ACCESS.2021.3072967, IEEE Access

II. BEARING DEGRADATION IN MULTI-PHASE PMSM CAUSED BY THE CMV

In general, the motor bearing faults are caused by two reasons, mechanical and electrical. Among the electrical reasons, the shaft current is a key factor. According to bearing manufacturers, 25% of the bearing faults are caused by the shaft current, and this ratio is rising with the development of power electronics devices [34].

When the voltage source inverter (VSI) is operated applying a conventional PWM method, the CMV is not zero, which induces the rotor voltage with the coupling effect of the internal parasitic capacitance of the motor. That rotor voltage provokes a common-mode current flow path with the motor bearing. As shown in Fig. 2, there are three types of parasitic capacitances in the motor: C_{wf} is the parasitic capacitance between the motor winding and stator core, C_{wr} is the lumped capacitor that represents the distributed effects from the windings to the rotor, and C_{rf} is the parasitic capacitance between the motor stator core and the rotor. Additionally, C_y is the dc-link to earth capacitance and R_g and L_g are the resistance and inductance of the ground path, respectively. C_b is the equivalent capacitance of the bearings on the drive side. Then, the bearing voltage u_b can be introduced with the effect of the parasitic capacitance [35].

The bearing faults caused by shaft current can be divided into four types [36]:

1) $\frac{\partial v}{\partial t}$ current, which are induced by the $\frac{\partial v}{\partial t}$ of the CMV. However, the influence of this fact is small.
2) EDM (Electric Discharge Machining) current. If the shaft voltage exceeds the threshold value of the oil film, the oil film will be broken down, resulting in the discharge phenomenon, which can cause the heat in the bearing and the corresponding lifetime can be reduced.
3) Circuital current, which is induced by the common-mode grounding current at high frequency. It can induce the high-frequency shaft voltage at both ends of the motor rotating shaft and generate the circulating bearing current.
4) Shaft to ground current when the motor frame is badly grounded, there will be voltage difference between the inner and outer rings of the bearing caused by rotor grounding or by driving load grounding.

Because of the EDM current, discharge occurs when the current passes through the bearing, which can increase the temperature of the bearing and bearing faults may occur. Therefore, reducing the shaft current is essential to increase lifetime and reliability of the motor system.

III. COMMON-MODE VOLTAGE (CMV) HARMONIC DESCRIPTION IN A DUAL DRIVE SYSTEM

Considering the model of Fig. 2, there is a common-mode path composed of the converter and the machine. Because both converters are connected to the motor frame through the parasitic capacitance and have the same dc-link, the equivalent common-mode voltage (CMV) of the two-converter system is the summation of the individual CMV of the VSIs as follows:

$$\begin{aligned} CMV &= V_{n_1O} + V_{n_2O} \\ &= \frac{V_{aO} + V_{bO} + V_{cO}}{3} + \frac{V_{a'O} + V_{b'O} + V_{c'O}}{3} \end{aligned} \quad (1)$$

To obtain an analytical expression of the resulting CMV in the six-phase machine, the double Fourier series expression is used. A periodical signal can be mathematically described as

$$\begin{aligned} x(t) &= \frac{A_{00}}{2} + \sum_{n=-\infty}^{\infty} \Big[A_{0n} \cos(n\omega_0 t) + B_{0n} \sin(n\omega_0 t) \Big] \\ &+ \sum_{m=1}^{\infty} \sum_{n=-\infty}^{\infty} \Big[A_{mn} \cos(m\omega_c + n\omega_0 t) \\ &+ B_{mn} \sin(m\omega_c + n\omega_0 t) \Big] \end{aligned} \quad (2)$$

where coefficient $A_{00}/2$ describe the average value of the signal, A_{0n} and B_{0n} correspond to the base-bands harmonic components, and A_{mn} and B_{mn} determine the side-bands harmonic components. Taking into account this fact and considering the traditional PWM approach, the phase voltage of phase x of a single VSI is determined as [8]:

$$\begin{aligned} V_{xO}(t) &= \frac{M_x V_{dc}}{2} \cos(\omega_0 t + \theta_x) \\ &+ \frac{2V_{dc}}{\pi} \sum_{m=1}^{\infty} \sum_{n=-\infty}^{\infty} \left[\frac{1}{m} J_n\left(\frac{m\pi}{2} M_x\right) \sin\left(\frac{(m+n)\pi}{2}\right) \right. \\ &\left. \cos\left(m\omega_c t + n\Big(\omega_0 t + \theta_x\Big)\right) \right] \end{aligned} \quad (3)$$

where indices m and n represents each side-band group (m) and each singular harmonic component inside the group (n). M_x is the modulation index of phase x ($x = a, b, c$) and θ_x is the phase displacement of the phase voltage in phase x. $J_n(z)$ is the first kind Bessel function of z and order n.

If the modulation indexes of all the phases in the VSI are the same, it is imposed that M_x=M. Also, it can be considered for the sake of simplicity that the phase displacement of phase a is $\theta_a = 0°$. Following these assumptions, the amplitude of the side-bands harmonics of the phase voltage V_{xO} of the a VSI can be mathematically described as:

$$V_{xO}(n,m) = \frac{2V_{dc}}{m\pi} J_n\left(\frac{m\pi}{2} M_x\right) \sin\left(\frac{(m+n)\pi}{2}\right) \quad (4)$$

As the key proposal of this work, in the dual drive system shown in Fig. 1, the phase displacement angle between the triangular carriers of the PWM methods in both VSIs of the dual drive system is considered a degree of freedom in order to improve the CMV of the overall system. In this sense, a phase displacement angle (φ) is considered in the triangular

This article has been accepted for publication in a future issue of this journal, but has not been fully edited. Content may change prior to final publication. Citation information: DOI 10.1109/ACCESS.2021.3072967, IEEE Access

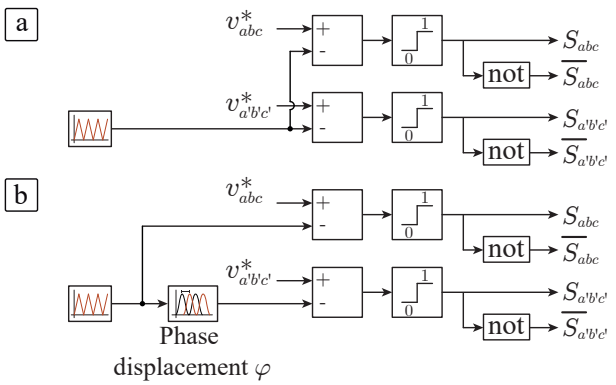

FIGURE 3: a) Traditional single-carrier PWM modulation for the three-phase two-level motor dual drive system b) Proposed multi-carrier modulation technique for the three-phase two-level motor dual drive system

carrier of the second VSI. Therefore, the phase voltages in second VSI system can be described, analogously to (3), as:

$$V_{x'O}(t) = \frac{M_{x'}V_{dc}}{2}\cos(\omega_0 t + \theta_{x'}) + \frac{2V_{dc}}{\pi}\sum_{m=1}^{\infty}\sum_{n=1}^{\infty}\left[\frac{1}{m}J_n\left(\frac{m\pi}{2}M_{x'}\right)\sin\left(\frac{(m+n)\pi}{2}\right)\cos\left(m\left(\omega_c t+\varphi\right)+n\left(\omega_0 t+\theta_{x'}\right)\right)\right] \quad (5)$$

where φ is the phase displacement of the carrier signal adopted for the second VSI with respect to the carrier signal adopted for the first one. $\theta_{x'}$ is the phase displacement of the phase voltage in phase x' ($x' = a', b', c'$). It can be observed that the amplitude of the side-bands harmonics of the phase voltage $V_{x'O}$ can be described similarly as was introduced in (4).

Taking into account these expressions, the resulting CMV in the six-phase machine can be determined as the summation of the CMV produced by both VSIs. More specifically, assuming the same value of the modulation index for all the phases (M=M_x=$M_{x'}$), each machine CMV side-bands harmonic component can be expressed by:

$$\begin{aligned} CMV(n,m) &= V_{n_1O}(n,m) + V_{n_2O}(n,m) \\ &= \frac{V_{dc}}{3m\pi}\sin\left((m+n)\frac{\pi}{2}\right)J_n\left(m\frac{\pi}{2}M\right)\cdot\left[\left[\left(1+e^{jn\theta_b}+e^{jn\theta_c}\right.\right.\right. \\ &+ \left.\left.\left.e^{j(m\varphi+n\theta_{a'})}+e^{j(m\varphi+n\theta_{b'})}+e^{j(m\varphi+n\theta_{c'})}\right)\right]e^{j(m\omega_c+n\omega_o)t} \\ &+ \left[\left(1+e^{-jn\theta_b}+e^{-jn\theta_c}+e^{-j(m\varphi+n\theta_{a'})}+e^{-j(m\varphi+n\theta_{b'})}\right.\right. \\ &+ \left.\left.e^{-j(m\varphi+n\theta_{c'})}\right)\right]e^{-j(m\omega_c+n\omega_o)t}\Bigg] \end{aligned} \quad (6)$$

In order to consider a wide frequency range in the resulting CMV, it is possible to consider the CMV Total Harmonic Distortion (THD) with respect to the half of the dc-Link as figure of merit.

$$THD_{CMV} = \frac{2}{V_{dc}}\sqrt{\sum_{m=1}^{N}\sum_{n=-j}^{j}CMV(n,m)^2} \quad (7)$$

where N and j are parameters that define respectively the number of harmonic groups and specific frequency components in each group included in the THD calculation.

Observing expression (7), it can be seen that the minimum value of the THD is always achieved with a carrier displacement angle φ equal to $180°$. In order to demonstrate this fact, in Fig 4a the THD has been calculated through simulation with a modulation index M equal to 0.4, 0.6 and 0.8. In this test, the multi-phase PMSM machine parameters are summarized in Table 1. The THD value has been calculated up to a maximum frequency of 9kHz where the frequency f_c in the triangular carriers of the PWM method are equal to 2kHz. Four complete harmonic groups (N=4) have been considered into the THD calculation, while j is fixed to 6.

In order to compare the impact of applying $\varphi = 180°$ in the PWM technique in the dual drive system, the CMV THD has been also computed for the whole modulation index range considering the conventional PWM method where both VSIs apply synchronized PWM methods ($\varphi = 0°$) (shown in Fig. 3a). Both modulation methods ($\varphi = 0°$ and $\varphi = 180°$) have been applied considering the scenario reported in Table 1. As can been observed in Fig. 4b, the PWM method with $\varphi = 180°$ is always superior achieving an important reduction of the CMV THD, specially with low values of the modulation index.

TABLE 1: Multi-phase PMSM parameters

Parameters	Values
Rated power $[kW]$	18
Rated current $[A]$	71
Rated speed $[rpm]$	3000
Pole pair number	4
Self inductance $[mH]$	0.347
Mutual inductance $[mH]$	-0.131
Phase resistance $[m\Omega]$	8.5
Back-EMF coefficient K_E	0.2506
Phase peak Back-EMF (at 25 Hz) $[V]$	9.84

Stator inductance matrix			
$L\ [mH]$	0.248	$M_0\ [mH]$	-0.099
$M_1\ [mH]$	-0.099	$M_2\ [mH]$	0.032

This article has been accepted for publication in a future issue of this journal, but has not been fully edited. Content may change prior to final publication. Citation information: DOI 10.1109/ACCESS.2021.3072967, IEEE Access

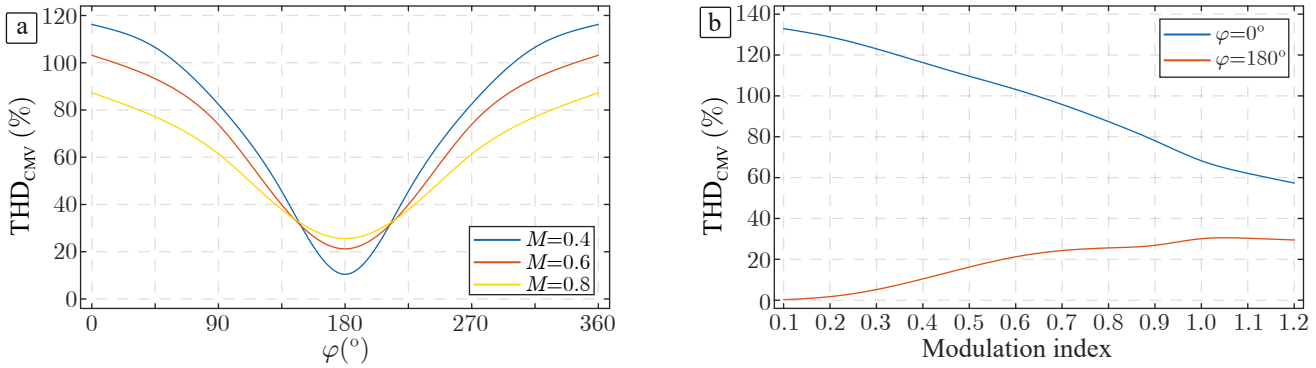

FIGURE 4: a) CMV THD value for a dual-drive system using the parameters reported in Table 1 with modulation index equal to 0.4, 0.6 and 0.8 b) CMV THD value for a dual-drive system using the parameters reported in Table 1 considering the traditional PWM technique ($\varphi = 0°$) and the phase-shifted PWM method with $\varphi = 180°$

IV. ANALYSIS OF THE CURRENT RIPPLE CONSIDERING THE PROPOSED CMV MITIGATION TECHNIQUE

Considering the dual three-phase PMSM machine shown in Fig. 1, the mathematical description of the stators winding is given by the its corresponding inductance matrix which is written as:

$$M_L = \begin{bmatrix} L & M_0 & M_0 & M_1 & M_2 & M_2 \\ M_0 & L & M_0 & M_2 & M_1 & M_2 \\ M_0 & M_0 & L & M_2 & M_2 & M_1 \\ M_1 & M_2 & M_2 & L & M_0 & M_0 \\ M_2 & M_1 & M_2 & M_0 & L & M_0 \\ M_2 & M_2 & M_1 & M_0 & M_0 & L \end{bmatrix} \quad (8)$$

where M_0, M_1, M_2 are real numbers.

Assuming an internal star connection of each subsystem and according to the current Kirchhoff Law, the currents through the windings fulfill that:

$$\begin{aligned} i_a + i_b + i_c &= 0 \\ i_{a'} + i_{b'} + i_{c'} &= 0 \end{aligned} \quad (9)$$

Neglecting the effect of low order back-EMF harmonics on current harmonics at high frequencies (i. e. the switching frequency and its superior multiples) and the voltage drop in the phase resistance, the relationship between high-frequency harmonic voltage (V_h) and high-frequency harmonic current (i_h) is determined by:

$$V_h = M_L \frac{di_h}{dt} \quad (10)$$

where V_h and i_h are defined as:

$$\begin{aligned} V_h &= \begin{bmatrix} V_{a,h} & V_{b,h} & V_{c,h} & V_{a',h} & V_{b',h} & V_{c',h} \end{bmatrix}^T \\ i_h &= \begin{bmatrix} i_{a,h} & i_{b,h} & i_{c,h} & i_{a',h} & i_{b',h} & i_{c',h} \end{bmatrix}^T \end{aligned} \quad (11)$$

Substituting (8) and (9) into (10), the harmonic voltage of the phase x ($x = a, b, c$) is determined by:

$$\begin{aligned} V_{x,h} &= (L + M_0)\frac{di_{x,h}}{dt} - (M_1 + M_2)\frac{di_{x',h}}{dt} \\ V_{x',h} &= (L + M_0)\frac{di_{x',h}}{dt} - (M_1 + M_2)\frac{di_{x,h}}{dt} \end{aligned} \quad (12)$$

Considering the CMV calculation and the analysis performed in section III, when the carriers of both VSIs are synchronized ($\varphi = 0°$) the phase voltages generated in both VSIs are identical and therefore, as $i_x = i'_x$, equation (12) can be rewritten as:

$$V_{x,h} = V_{x',h} = (L + M_0 - M_1 - M_2)\frac{di_{x,h}}{dt} \quad (13)$$

On the contrary, considering the CMV mitigation technique proposed in section III by fixing a carrier phase displacement between both VSIs equal to $\varphi = 180°$, it is fulfilled that $i_x = -i_{x'}$. In this case, the phase voltages can be described as:

$$V_{x,h} = -V_{x',h} = (L + M_0 + M_1 + M_2)\frac{di_{x,h}}{dt} \quad (14)$$

Then, through direct comparison between (13) and (14), a higher impedance value results in the whole system when a carrier phase displacement between both VSIs equal to 180° is applied. As a consequence of this higher impedance, the ripple of the current present in the system is reduced.

V. EXPERIMENTAL RESULTS

In order to validate the harmonic analysis and the effectiveness of the proposed modulation technique, the downscaled laboratory experimental setup shown in Fig. 5 has been considered. The prototype consists of a dual three-phase two-level VSDs connected to a dual-phase PMSM machine. Each single three-phase VSI is built using the IGBT IKW75N60T by Infineon Technologies [37]. Figure 6 shows the PMSM control strategy based on the traditional FOC

This article has been accepted for publication in a future issue of this journal, but has not been fully edited. Content may change prior to final publication. Citation information: DOI 10.1109/ACCESS.2021.3072967, IEEE Access

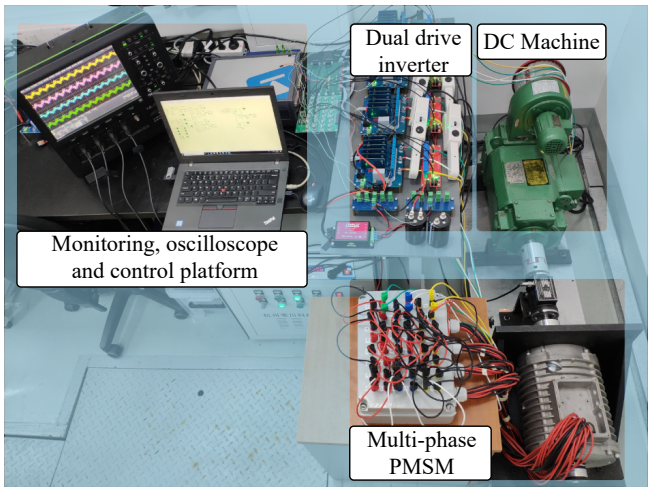

FIGURE 5: Experimental laboratory prototype of the dual VSD connected to a multi-phase PMSM

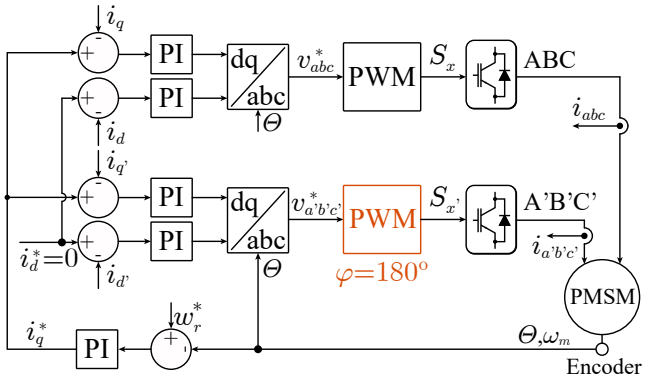

FIGURE 6: FOC control strategy implemented in the experimental setup including the phase displacement between the PWM methods ($\varphi = 180°$)

strategy including the proposed CMV reduction method. In this sense, the PMSM is driven by a speed and current double closed control loop. This controller scheme as well as the modulation techniques have been implemented using a rapid control prototype platform PLECS RT box [38]. The details of the multi-phase PMSM machine are listed in Table 1. The operation of the PMSM is analyzed in terms of the total CMV generated applying both modulation method approaches and the results are included in Fig. 7. Because of some limitations present experimental setup to drive the machine, the experiments has been performed considering a reduced dc-link voltage equal to 40V, a switching frequency of 4kHz and a speed reference of 600rpm.

The total generated CMV applying the traditional modulation technique with synchronized PWM methods in both VSDs ($\varphi = 0°$) is represented in Fig. 7a and its harmonic spectrum is shown in Fig. 7b considering also a zoomed detail of the distortion at the carrier frequency and its multiples in Fig. 7c. As it is clearly shown, there is a non-negligible harmonic component located at the switching frequency

TABLE 2: THD values considering up to 30kHz

		THD_{CMV} [%]		Phase current *THD*[%]	
Speed (rpm)	Modulation index	Traditional PWM ($\varphi = 0°$)	Proposed PWM ($\varphi = 180°$)	Traditional PWM ($\varphi = 0°$)	Proposed PWM ($\varphi = 180°$)
200	0.27	126.62	9.60	12.87	10.10
400	0.48	114.78	18.38	25.26	18.60
600	0.67	101.52	23.20	34.18	20.48

(with an approximately a magnitude of 50%) and at its multiples as well. On the other hand, the proposed technique applying a 180° carrier phase displacement between both VSIs is also tested considering the same FOC strategy as well as the same operational conditions in the machine. As it can be observed in Fig. 7d, the peak-to-peak CMV has been considerably reduced compared with that represented in Fig. 7a. In addition, in Fig. 7e is represented a detail of the resulting time-variant CMV. These narrow pulses are provoked, among other reasons, because of the dead time imposed by the IGBT driver circuit in the pulses generated by each VSI. However, as it is illustrated in Fig. 7f, the first (and third) harmonic groups of the resulting CMV harmonic spectrum have been eliminated while the second harmonic group remains unaltered as shown in Fig. 7f.

The operation of the PMSM has been also analyzed in terms of the obtained phase currents and the corresponding experimental results are represented in Fig. 8. Following the discussion addressed in section IV, the currents obtained by applying the proposed PWM strategy with $\varphi = 180°$ present a better performance because of the harmonic reduction in high-frequency components. Through a direct comparison between Fig. 8c and Fig. 8f, it is possible to observe this improvement as a harmonic mitigation at switching frequency as well as the third carrier-order harmonic content. As it happens with the CMV, the harmonic content located in the second harmonic group remains unaltered.

In order to test the proposed PWM strategy with different operational conditions, these experiments have been carried out with different PMSM reference speeds. The resulting harmonic distortion of the total CMV as well as the phase currents THD data, considering up to 9kHz have been summarized in Table 2. As it can be seen from the results, the proposed total CMV mitigation method achieves superior results as expected from the analysis introduced in section III. Additionally, the resulting phase currents THD values are also reduced as expected from the discussion provided in section IV. It is important to notice that each rotational speed corresponds to an specific modulation index value because the FOC method shown in Fig. 6 determines the reference voltages to be generated by the VSDs in order to track the speed. It is important to highlight that the obtained results fit well with the expected results determined by simulation and shown in Fig. 4b. The results summarized in Table 2 are just three examples to show this fact.

This article has been accepted for publication in a future issue of this journal, but has not been fully edited. Content may change prior to final publication. Citation information: DOI 10.1109/ACCESS.2021.3072967, IEEE Access

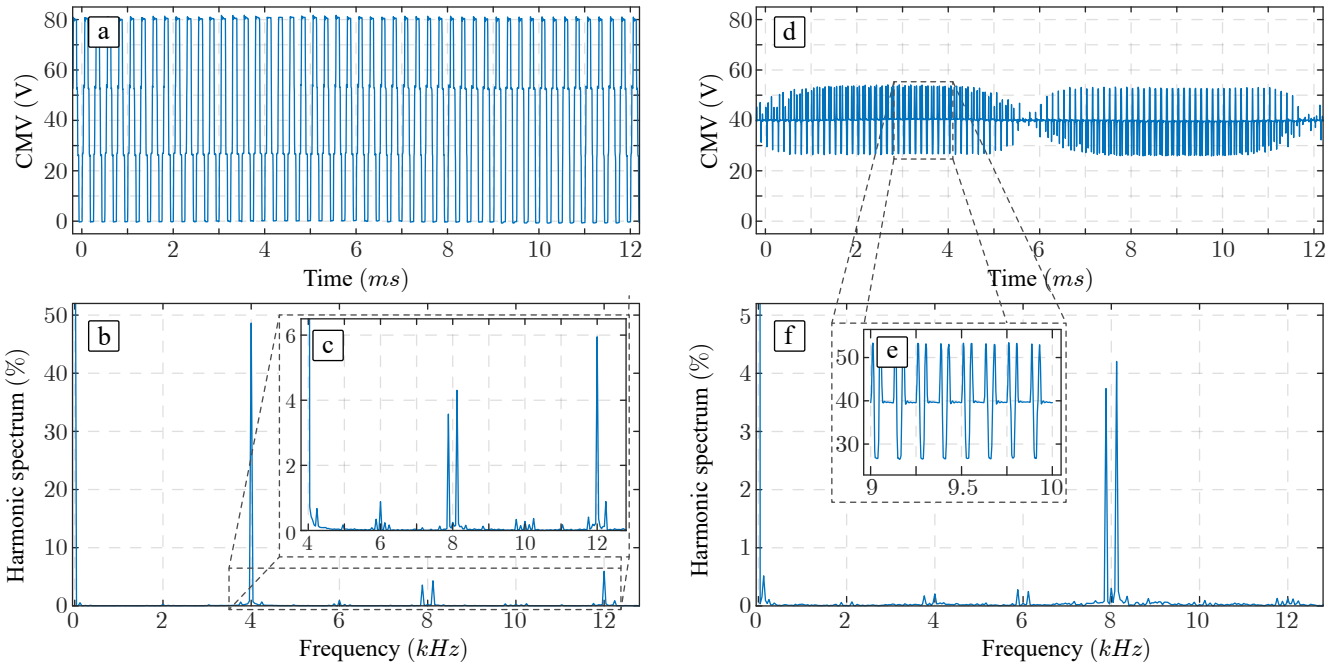

FIGURE 7: Results applying the traditional PWM method with synchronized carriers ($\varphi = 0°$) in both VSIs a) Total CMV b) CMV harmonic spectrum c) Detail of the CMV harmonic spectrum. Results applying the proposed modulation method with carrier phase displacement between the VSIs equal to $\varphi = 180°$ d) Total CMV e) Detail of the total CMV f) CMV harmonic spectrum

VI. IMPACT OF THE RESULTING CMV OVER LEAKAGE CURRENT AND SHAFT VOLTAGE

As it was addressed in section II, the introduction of high frequency CMV content accelerates the bearing degradation because of the mentioned leakage currents and shaft voltage. In this sense, due to the impossibility of measuring these magnitudes in the experimental setup, the impact over the leakage current as well as the shaft voltage has been determined using a specialized simulation environment considering the parasitic model shown in Fig. 9 and the measured CMV shown in Fig. 7 for both modulation techniques. This electrical model has been conducted following the work presented in [22].

In this sense, the common-mode circuit of the machine winding is composed by an inductive (L) plus resistive (R_s) components. Moreover, the parallel parasitic resistance of the winding (due to insulation) is also considered with a lumped resistor R_p. Additionally, there are two capacitive paths from the windings to the frame which are represented by C_{wf} and the second path closes through the rotor and represented by C_{wr}. The first one is the capacitance between the windings and the frame whereas the second is the capacitance between the winding and the rotor. A voltage across the rotor and the frame appears (so-called shaft voltage) and it is an well-known indicator regarding the bearing lifespan.

Additionally, some extra capacitive components are required to be introduced. C_{rf} is the capacitance between rotor and the frame and C_b is the capacitance due to the bearings. The current that flows through this capacitance is responsible for the bearing degradation. The other parameters regards the earth connection: R_g and L_g are resistance and inductance of the path connecting the frame of the machine to the earth point of the converter and C_g represents the high-voltage capacitors that are usually connected between the dc-link of the converter and earth. The value of the parameters can change depending on the type of the machine (a reduced air-gap, for instance, reduces the C_{wf}), however it is always true that a reduced CMV excitation reduces the current through C_b. The corresponding circuit parameters for the experimental setup are properly listed in Fig. 9.

On one hand, it is possible to calculate the induced shaft voltage in the machine by the application of both modulation strategies. The obtained results are shown in Fig. 11. As it can be observed, the application of the conventional modulation technique with $\varphi = 0°$ leads to relatively large shaft voltage as shown in Fig. 11a. If the harmonic spectrum is represented, there is a non-negligible dc component as well as the magnitude of the first and third harmonic groups are high as shown in Fig. 11b. On the contrary, as it is presented in Fig. 11b and Fig. 11d, after the application of the proposed modulation technique with $\varphi = 180°$, not only the peak-to-peak magnitude of the shaft voltage is reduced but the dc component is eliminated as well as the first and third harmonic groups are greatly mitigated. These results completely fit with the experimental results presented for the CMV reduction.

On the other hand, the leakage current has been also calcu-

This article has been accepted for publication in a future issue of this journal, but has not been fully edited. Content may change prior to final publication. Citation information: DOI 10.1109/ACCESS.2021.3072967, IEEE Access

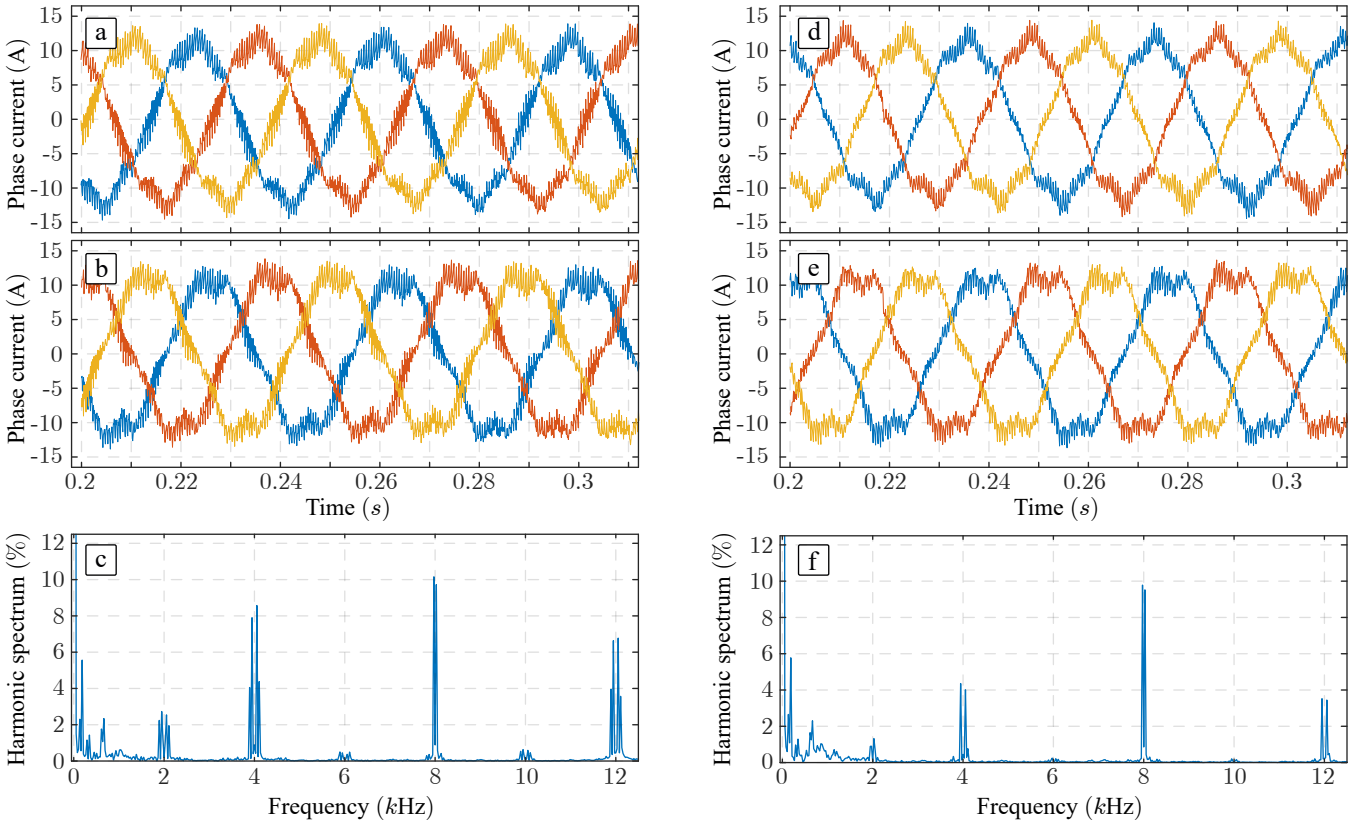

FIGURE 8: Results applying the traditional PWM method with synchronized carriers (($\varphi = 0°$)) in both VSIs a) Phase currents of drive 1 b) Phase currents of drive 2 c) Harmonic spectrum of current in phase a. Results applying the proposed PWM method with carrier phase displacement between the VSIs equal to $\varphi = 180°$ d) Phase currents of drive 1 e) Phase currents of drive 2 f) Harmonic spectrum of current in phase a

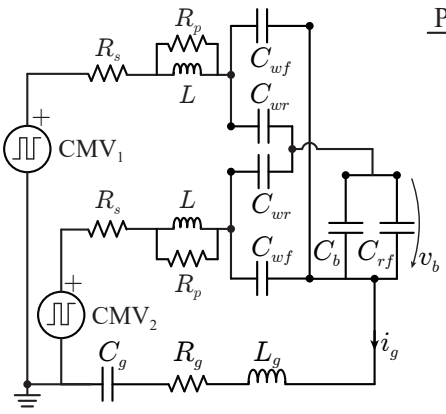

Parameter values	
R_s	$= 2.83\Omega$
R_p	$= 10k\Omega$
L	$= 115.6\mu$H
C_b	$= 590p$F
C_{rf}	$= 1.66n$F
C_{wf}	$= 3n$F
C_{wr}	$= 1p$F
L_g	$= 10\mu$H
R_g	$= 0.1\Omega$
C_g	$= 4n$F

FIGURE 9: Circuit parameters for the modeling of the parasitic effects of the experimental setup shown in Fig. 5

lated using the simulation model and similar conclusions can be drawn as it is shown in Fig. 10.

From these results, it can be concluded that the proposed modulation technique presents a positive impact in the operation of the machine since the resulting CMV is mitigated and therefore, the induced shaft voltage and the leakage current are also minimized.

VII. CONCLUSIONS

The use of multiphase machines being operated by several converters connected to the same dc-link is nowadays an attractive solution for many motor drive applications. However, VSDs for motor drives present inherent problems related to the reliability of the complete power system. As a main issue, the motor bearing degradation because of the presence of CMV in the VSD is actually a challenge to be overcome. Among the solutions previously provided by literature, many active canceler, passive filtering techniques and some SVM-based modulation methods have been proposed to achieve the mitigation of the CMV.

This paper proposes a simple carrier phase displacement between the PWM methods of a dual VSD to mitigate the resulting CMV harmonic content. The simplicity of the proposed method is outstanding compared with previous methods based on SVM strategies. This technique does not require the usage of any external active or passive element and it is easily implementable in most of the digital control platforms. In order to validate theoretically the proposed method, a detailed mathematical model based on double Fourier series of the phase voltages and currents has been

This article has been accepted for publication in a future issue of this journal, but has not been fully edited. Content may change prior to final publication. Citation information: DOI 10.1109/ACCESS.2021.3072967, IEEE Access

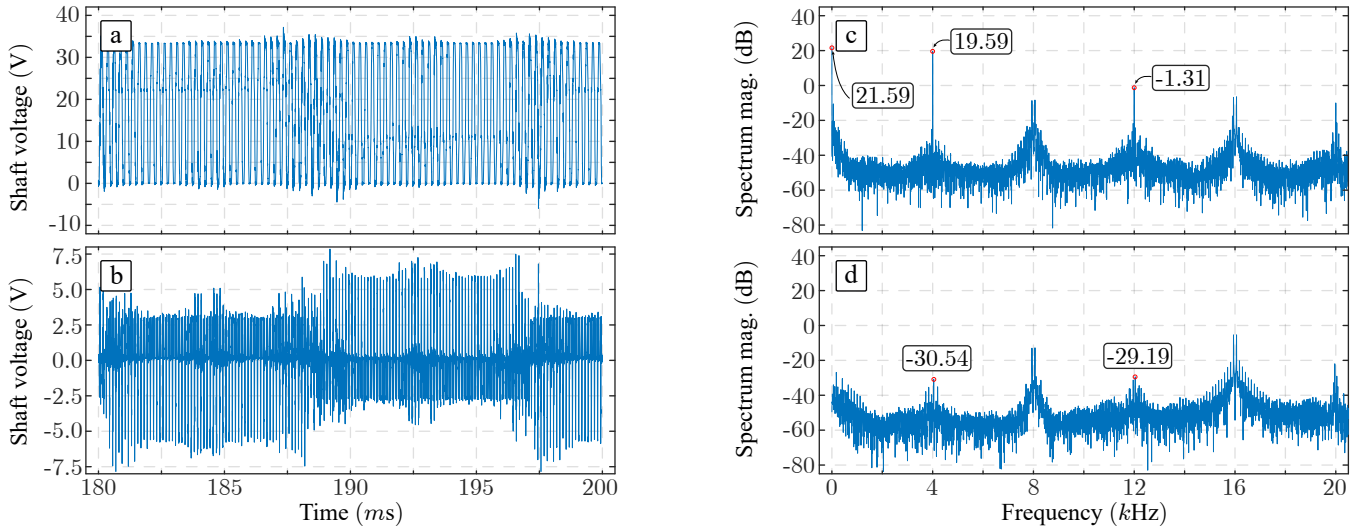

FIGURE 10: Resulting shaft voltage from simulation circuit presented in Fig. 9. a) Conventional modulation method b) Proposed modulation method c) Harmonic spectrum for conventional modulation method d) Harmonic spectrum for proposed modulation method

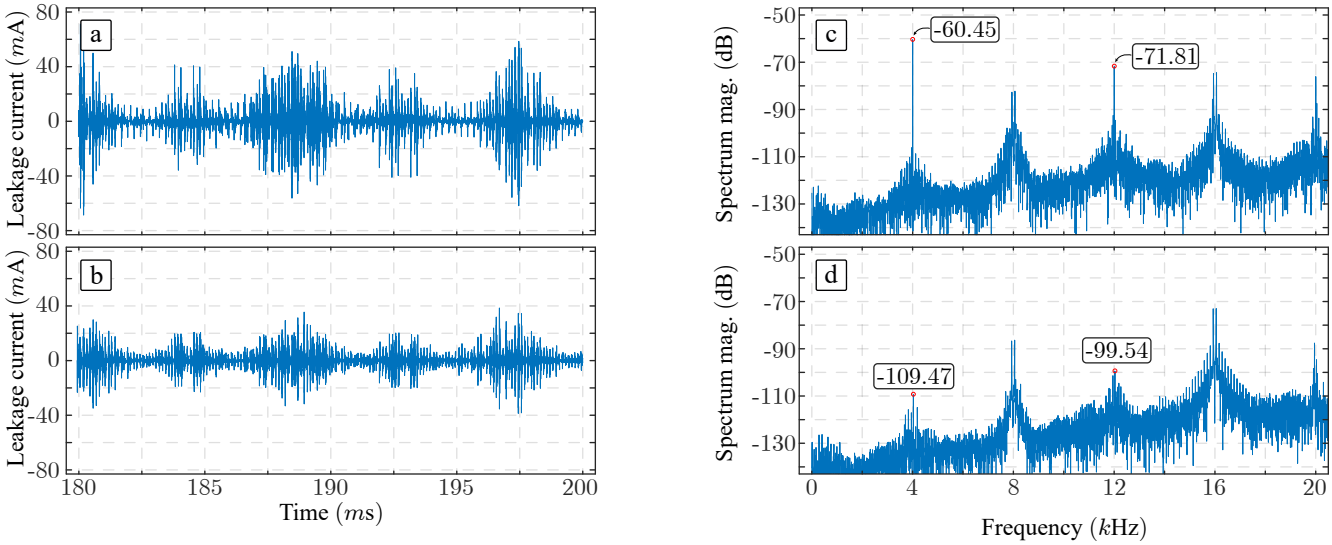

FIGURE 11: Resulting leakage current from simulation circuit presented in Fig. 9 applying a) the conventional modulation method b) the proposed modulation method. Leakage current harmonic spectrum applying c) the conventional modulation method d) the proposed modulation method

provided. From this analysis, it is demonstrated that the best result is achieved when the carrier phase displacement between both VSIs of the dual drive is fixed to $\varphi = 180°$. The proposed PWM technique has been tested in a down-scaled dual PMSM machine considering different scenarios achieving a superior performance. The impact on the leakage currents and the shaft voltage has been also evaluated. The results demonstrate that a superior system performance is achieved.

REFERENCES

[1] G. Buticchi, S. Bozhko, M. Liserre, P. Wheeler, and K. Al-Haddad, "On-board microgrids for the more electric aircraft-technology review," *IEEE Transactions on Industrial Electronics*, vol. 66, no. 7, pp. 5588–5599, July 2019.

[2] Z. Wang, J. Chen, M. Cheng, and K. T. Chau, "Field-oriented control and direct torque control for paralleled vsis fed pmsm drives with variable switching frequencies," *IEEE Transactions on Power Electronics*, vol. 31, no. 3, pp. 2417–2428, March 2016.

[3] H. Yang, R. Yang, W. Hu, and Z. Huang, "Fpga-based sensorless speed control of pmsm using enhanced performance controller based on the reduced-order ekf," *IEEE Journal of Emerging and Selected Topics in Power Electronics*, pp. 1–1, 2019.

[4] H. S. Che, E. Levi, M. Jones, W. Hew, and N. A. Rahim, "Current control methods for an asymmetrical six-phase induction motor drive," *IEEE*

Transactions on Power Electronics, vol. 29, no. 1, pp. 407–417, Jan 2014.

[5] Y. Luo and C. Liu, "Elimination of harmonic currents using a reference voltage vector based-model predictive control for a six-phase pmsm motor," *IEEE Transactions on Power Electronics*, vol. 34, no. 7, pp. 6960–6972, July 2019.

[6] P. Xu, J. H. Feng, S. Y. Guo, S. Feng, W. Chu, Y. Ren, and Z. Q. Zhu, "Analysis of dual three-phase permanent-magnet synchronous machines with different angle displacements," *IEEE Transactions on Industrial Electronics*, vol. 65, no. 3, pp. 1941–1954, March 2018.

[7] E. Levi, "Multiphase electric machines for variable-speed applications," *IEEE Transactions on Industrial Electronics*, vol. 55, no. 5, pp. 1893–1909, 2008.

[8] D. G. Holmes and T. A. Lipo. Wiley-IEEE Press, 2003, pp. 744–. [Online]. Available: http://ieeexplore.ieee.org/xpl/articleDetails.jsp?arnumber=5311953

[9] P. K. V. Kunisetti and T. V. Kumar, "Enhanced direct torque control and predictive torque control strategies of an open-end winding induction motor drive to eliminate common-mode voltage and weighting factors," *IET Power Electronics*, vol. 12, no. 8, pp. 1986–1997, 2019.

[10] J. I. Leon, S. Kouro, L. G. Franquelo, J. Rodriguez, and B. Wu, "The essential role and the continuous evolution of modulation techniques for voltage-source inverters in the past, present, and future power electronics," *IEEE Transactions on Industrial Electronics*, vol. 63, no. 5, pp. 2688–2701, May 2016.

[11] J. I. Leon, S. Vazquez, and L. G. Franquelo, "Multilevel converters: Control and modulation techniques for their operation and industrial applications," *Proceedings of the IEEE*, vol. 105, no. 11, pp. 2066–2081, Nov 2017.

[12] S. Vazquez, J. Rodriguez, M. Rivera, L. G. Franquelo, and M. Norambuena, "Model predictive control for power converters and drives: Advances and trends," *IEEE Transactions on Industrial Electronics*, vol. 64, no. 2, pp. 935–947, Feb 2017.

[13] G. Feng, C. Lai, M. Kelly, and N. C. Kar, "Dual three-phase pmsm torque modeling and maximum torque per peak current control through optimized harmonic current injection," *IEEE Transactions on Industrial Electronics*, vol. 66, no. 5, pp. 3356–3368, May 2019.

[14] D. Eaton, J. Rama, and P. Hammond, "Neutral shift [five years of continuous operation with adjustable frequency drives]," *IEEE Industry Applications Magazine*, vol. 9, no. 6, pp. 40–49, Nov 2003.

[15] J. Kalaiselvi and S. Srinivas, "Bearing currents and shaft voltage reduction in dual-inverter-fed open-end winding induction motor with reduced cmv pwm methods," *IEEE Transactions on Industrial Electronics*, vol. 62, no. 1, pp. 144–152, Jan 2015.

[16] A. Mutzw, "Thousands of hits: on inverter-induced bearing currents, related work, and the literature," *Elektrotechnik und Informationstechnik*, vol. 128, no. 11, pp. 382–388, Dic 2011.

[17] A. M. Hava and E. Un, "A high-performance pwm algorithm for common-mode voltage reduction in three-phase voltage source inverters," *IEEE Transactions on Power Electronics*, vol. 26, no. 7, pp. 1998–2008, July 2011.

[18] Y. Isomura, K. Yamamoto, S. Morimoto, T. Maetani, A. Watanabe, and K. Nakano, "Study of the further reduction of shaft voltage of brushless dc motor with insulated rotor driven by pwm inverter," *IEEE Transactions on Industry Applications*, vol. 50, no. 6, pp. 3738–3743, Nov 2014.

[19] D. Jiang, J. Chen, and Z. Shen, "Common mode emi reduction through pwm methods for three-phase motor controller," *CES Transactions on Electrical Machines and Systems*, vol. 3, no. 2, pp. 133–142, June 2019.

[20] R. Naik, T. A. Nondahl, M. J. Melfi, R. Schiferl, and Jian-She Wang, "Circuit model for shaft voltage prediction in induction motors fed by pwm-based ac drives," *IEEE Transactions on Industry Applications*, vol. 39, no. 5, pp. 1294–1299, Sep. 2003.

[21] J. Song-Manguelle, S. SchrÃ¶der, T. Geyer, G. Ekemb, and J. Nyobe-Yome, "Prediction of mechanical shaft failures due to pulsating torques of variable-frequency drives," *IEEE Transactions on Industry Applications*, vol. 46, no. 5, pp. 1979–1988, Sep. 2010.

[22] O. Magdun and A. Binder, "High-frequency induction machine modeling for common mode current and bearing voltage calculation," *IEEE Transactions on Industry Applications*, vol. 50, no. 3, pp. 1780–1790, May 2014.

[23] H. M. Flieh, E. Totoki, and R. D. Lorenz, "Dynamic shaft torque observer structure enabling accurate dynamometer transient loss measurements," *IEEE Transactions on Industry Applications*, vol. 54, no. 6, pp. 6121–6132, Nov 2018.

[24] C. Choochuan, "A survey of output filter topologies to minimize the impact of pwm inverter waveforms on three-phase ac induction motors," vol. 2005, 01 2005, pp. 1 – 544.

[25] Chenggang Mei, J. C. Balda, and W. P. Waite, "Cancellation of common-mode voltages for induction motor drives using active method," *IEEE Transactions on Energy Conversion*, vol. 21, no. 2, pp. 380–386, June 2006.

[26] K. Jayaraman and M. Kumar, "Design of passive common-mode attenuation methods for inverter-fed induction motor drive with reduced common-mode voltage pwm technique," *IEEE Transactions on Power Electronics*, vol. 35, no. 3, pp. 2861–2870, March 2020.

[27] R. M. Tallam, R. J. Kerkman, D. Leggate, and R. A. Lukaszewski, "Common-mode voltage reduction pwm algorithm for ac drives," *IEEE Transactions on Industry Applications*, vol. 46, no. 5, pp. 1959–1969, Sep. 2010.

[28] D. Han, C. T. Morris, and B. Sarlioglu, "Common-mode voltage cancellation in pwm motor drives with balanced inverter topology," *IEEE Transactions on Industrial Electronics*, vol. 64, no. 4, pp. 2683–2688, 2017.

[29] J. Espina, C. Ortega, L. de Lillo, L. Empringham, J. Balcells, and A. Arias, "Reduction of output common mode voltage using a novel svm implementation in matrix converters for improved motor lifetime," *IEEE Transactions on Industrial Electronics*, vol. 61, no. 11, pp. 5903–5911, Nov 2014.

[30] P. Hollstegge, A. Wanke, and R. W. De Doncker, "Noise mitigation in dual three-phase internal permanent magnet machines by injection of current harmonics," *The Journal of Engineering*, vol. 2019, no. 17, pp. 4273–4277, 2019.

[31] W. Hu, C. Ruan, H. Nian, and D. Sun, "Zero-sequence current suppression strategy with common-mode voltage control for open-end winding pmsm drives with common dc bus," *IEEE Transactions on Industrial Electronics*, vol. 68, no. 6, pp. 4691–4702, 2021.

[32] M. Mekasser, Q. Gao, and C. Xu, "Common mode voltage elimination in dual-inverter-fed six-phase open-end winding pmsm drives with a single dc supply," *The Journal of Engineering*, vol. 2019, no. 17, pp. 3598–3602, 2019.

[33] Z. Shen, D. Jiang, Z. Liu, D. Ye, and J. Li, "Common-mode voltage elimination for dual two-level inverter-fed asymmetrical six-phase pmsm," *IEEE Transactions on Power Electronics*, vol. 35, no. 4, pp. 3828–3840, April 2020.

[34] A. Romanenko, A. Muetze, and J. Ahola, "Incipient bearing damage monitoring of 940-h variable speed drive system operation," *IEEE Transactions on Energy Conversion*, vol. 32, no. 1, pp. 99–110, March 2017.

[35] S. Lee, J. Park, C. Jeong, S. Rhyu, and J. Hur, "Shaft-to-frame voltage mitigation method by changing winding-to-rotor parasitic capacitance of ipmsm," *IEEE Transactions on Industry Applications*, vol. 55, no. 2, pp. 1430–1436, March 2019.

[36] A. Muetze and A. Binder, "Techniques for measurement of parameters related to inverter-induced bearing currents," *IEEE Transactions on Industry Applications*, vol. 43, no. 5, pp. 1274–1283, Sep. 2007.

[37] Ikw75n60t datasheet. [Online]. Available: https://www.infineon.com/

[38] Plexim rt box rapid prototype platform. [Online]. Available: https://www.plexim.com/

ABRAHAM MARQUEZ (S'14-M'16) was born in Huelva, Spain, in 1985. He received his B.S., M.S. and Ph.D degrees in telecommunications engineering from Universidad de Sevilla (US), Seville, Spain in 2014, 2016 and 2019, respectively. His main research interest are modulation techniques, multilevel converters, model-based predictive control of power converters and drives, renewable energy sources, and power devices lifetime extension. Dr. Marquez was recipient as coauthor of the 2015 Best Paper Award of the IEEE Industrial Electronics Magazine.

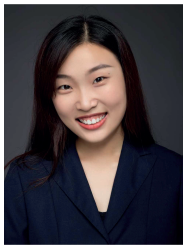

XUCHEN WANG (S'19) was born in Taizhou, China, in 1993. She received her B.Eng. (Hons.) degree in electrical and electronic engineering from the University of Nottingham Ningbo China in 2015. In 2019, she obtained the Ph.D. degree from the University of Nottingham in Electrical Engineering. She is currently a researcher with the department of electrical and electronic engineering (PEMC group), at the University of Nottingham. Her research interests include design, modelling and control of multiphase drives.

HAO YAN (M'18) received the B.S., M.S. and Ph.D. degrees in electrical engineering from the Harbin Institute of Technology, Harbin, China, in 2011, 2013 and 2018, respectively. From 2017 to 2019, he joined the Power Electronics, Machines and Control Group, University of Nottingham, Ningbo, China, and worked on power electronics for electrical drives. From 2019 to 2020, he was a Research Fellow with the with the Rolls-Royce @ NTU Corporate Lab, Nanyang Technological University, Singapore 639798. He is currently an Associate Professor with the School of Civil Aviation, Northwestern Polytechnical University, Xi'an, China. His current research interests include permanent-magnet machine drives and power converters in More Electric Aircraft.

JOSE I. LEON (Fellow, IEEE) (S'04-M'07-SM'14-F'17) was born in Cadiz, Spain. He received the B.S., M.S., and PhD degrees in telecommunications engineering from Universidad de Sevilla (US), Seville, Spain, in 1999, 2001, and 2006, respectively. Currently, he is an Associate Professor with the Department of Electronic Engineering, US. Since 2019 he is also Chair Professor at the Department of Control Science and Engineering in Harbin Institute of Technology (China).

His research interests include modulation and control of power converters for high-power applications and renewable energy systems. Dr. Leon was a co-recipient of the 2008 Best Paper Award of IEEE Industrial Electronics Magazine, the 2012 Best Paper Award of the IEEE Transactions on Industrial Electronics, and the 2015 Best Paper Award of IEEE Industrial Electronics Magazine. He was the recipient of the 2014 IEEE J. David Irwin Industrial Electronics Society Early Career Award, the 2017 IEEE Bimal K. Bose Energy Systems Award and the 2017 Manuel Losada Villasante Award for excellence in research and innovation. In 2017 he was elevated to the IEEE fellow grade with the following citation "for contributions to high-power electronic converters".

VITO GIUSEPPE MONOPOLI (S'98-M'05-SM'18) received the M.Sc. and Ph.D. degrees in electrical engineering from the Bari Polytechnic, in 2000 and 2004, respectively. He is currently an Assistant Professor Bari Polytechnic, Bari, Italy. His research activity concerns multilevel converters and the analysis of harmonic distortion produced by power converters and electrical drives. He is particularly interested in innovative control techniques for power converters. He is member of the IEEE Industry Applications Society, IEEE Industrial Electronics Society and IEEE Power Electronics Society.

GIAMPAOLO BUTICCHI (SM'17) received the Master degree in Electronic Engineering in 2009 and the Ph.D degree in Information Technologies in 2013 from the University of Parma, Italy. In 2012 he was visiting researcher at The University of Nottingham, UK. Between 2014 and 2017, he was a post-doctoral researcher, and Guest Professor at the University of Kiel, Germany. During his stay in Germany, he was awarded with the Von Humboldt Post-doctoral Fellowship to carry out research related to fault tolerant topologies of smart transformers.

In 2017 he was appointed as Associate Professor in Electrical Engineering at The University of Nottingham Ningbo China and as Head of Power Electronics of the Nottingham Electrification Center. He was promoted to Professor in 2020. His research focuses on power electronics for renewable energy systems, smart transformer fed micro-grids and dc grids for the More Electric Aircraft. Dr. Buticchi is one of the advocates for DC distribution systems and multi-port power electronics onboard the future aircraft.

He is author/co-author of more than 210 scientific papers, an Associate Editor of the IEEE Transactions on Industrial Electronics, the IEEE Transactions on Transportation Electrification and the IEEE Open Journal of the Industrial Electronics Society. He is currently the Chair of the IEEE Industrial Electronics Society Technical Committee on Renewable Energy Systems.

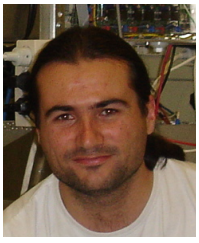

SERGIO VAZQUEZ (S'04, M'08, SM'14) was born in Seville, Spain, in 1974. He received the M.S. and PhD degrees in industrial engineering from the University of Seville (US) in 2006, and 2010, respectively.

Since 2002, he is with the Power Electronics Group working in R&D projects. He is an Associate Professor with the Department of Electronic Engineering, US. His research interests include power electronics systems, modeling, modulation and control of power electronics converters applied to renewable energy technologies.

Dr. Vazquez was recipient as coauthor of the 2012 Best Paper Award of the IEEE Transactions on Industrial Electronics and 2015 Best Paper Award of the IEEE Industrial Electronics Magazine. He is involved in the Energy Storage Technical Committee of the IEEE industrial electronics society and is currently serving as an Associate Editor of the IEEE Transactions on Industrial Electronics.

This article has been accepted for publication in a future issue of this journal, but has not been fully edited. Content may change prior to final publication. Citation information: DOI 10.1109/ACCESS.2021.3072967, IEEE Access

MARCO LISERRE (S'00-M'02-SM'07-F'13) received the MSc and PhD degree in Electrical Engineering from the Bari Polytechnic, respectively in 1998 and 2002. He has been Associate Professor at Bari Polytechnic and Professor in reliable power electronics at Aalborg University (Denmark). He is currently Full Professor and he holds the Chair of Power Electronics at Christian-Albrechts-University of Kiel (Germany). He has published over 300 technical papers (more than 100 of them in international peerreviewed journals), 4 chapters of a book and a book (Grid Converters for Photovoltaic and Wind Power Systems, ISBN-10: 0-470-05751-3 - IEEE-Wiley, second reprint, also translated in Chinese). These works have received more than 20000 citations. Marco Liserre is listed in ISI Thomson report "The world?s most influential scientific minds" from 2014.He has been awarded with an ERC Consolidator Grant for the project "The Highly Efficient And Reliable smart Transformer (HEART), a new Heart for the Electric Distribution System". He is member of IAS, PELS, PES and IES. He is Associate Editor of the IEEE Transactions on Industrial Electronics, IEEE Industrial Electronics Magazine, IEEE Transactions on Industrial Informatics, where he is currently Co-Eic, IEEE Transactions on power electronics and IEEE Journal of Emerging and Selected Topics in Power Electronics. He has been Founder and Editor-in-Chief of the IEEE Industrial Electronics Magazine, Founder and the Chairman of the Technical Committee on Renewable Energy Systems, Co-Chairman of the International Symposium on Industrial Electronics (ISIE 2010), IES Vice-President responsible of the publications. He has received the IES 2009 Early Career Award, the IES 2011 Anthony J. Hornfeck Service Award, the 2014 Dr. Bimal Bose Energy Systems Award, the 2011 Industrial Electronics Magazine best paper award and the Third Prize paper award by the Industrial Power Converter Committee at ECCE 2012, 2012. He is senior member of IES AdCom. In 2013 he has been elevated to the IEEE fellow grade with the following citation "for contributions to grid connection of renewable energy systems and industrial drives".

LEOPOLDO G. FRANQUELO (M'84-SM'96-F'05) was born in Malaga, Spain. He received the M.Sc. and Ph.D. degrees in electrical engineering from the Universidad de Sevilla, Seville, Spain, in 1977 and 1980, respectively. He was associate professor from 1982-86 at the Electronics Engineering Department in Sevilla University and currently is professor at the Electronics Engineering Department in Sevilla University since 1986 and a 1000 Talent Professor at the Department of Control Science and Engineering in Harbin Institute of Technology since 2016. His current research interests include modulation techniques for multilevel inverters and application to power electronic systems for renewable energy systems. He has participated in more than 100 Industrial and R&D projects and has published more than 300 papers, 76 of them in IEEE Journals. Dr. Franquelo is an IEEE Fellow since 2005 and an IEEE Industrial Electronics Society (IES) Distinguished Lecturer since 2006. In the IEEE TRANSACTIONS ON INDUSTRIAL ELECTRONICS, he became an Associate Editor in 2007, Co-Editor-in-Chief in 2014, and the Editor-in-Chief since 2016. He was a Member-at-Large of the IES AdCom (2002?2003), Vice President for Conferences (2004?2007), and President Elect of the IES (2008?2009). He was the President of the IES (2010?2011) and is an IES AdCom Life member. In 2009 and 2013, he received the prestigious Andalusian Research Award and FAMA Award recognizing the excellence of his research career. He has received a number of Best Paper Awards from IEEE journals. In 2012 and 2015, he was the recipient of the Eugene Mittelmann Outstanding Research Achievement Award and the Antohny J. Hornfeck Service Award from IEEE-IES, respectively.